Synthesis and Characterization of a Poly(styrene-*block*-methylacrylate-*random*-octadecylacrylate-*block*-styrene) Shape Memory ABA Triblock Copolymer

Pengzhan Fei and Kevin A. Cavicchi*

The Department of Polymer Engineering, The University of Akron, Akron, Ohio 44325-0301

ABSTRACT A new shape memory polymer (SMP) was prepared from an ABA triblock copolymer with polystyrene (PS) end blocks and a random copolymer midblock of poly(methylacrylate-*random*-octadecylacrylate) (PMA-*r*-PODA). The self-assembly of the triblock copolymer generates a three-dimensional, physically cross-linked network by the bridging of the midblocks across the glassy PS domains, which is used as the permanent network in the SMP. A second reversible network is generated by the side-chain crystallization of the PODA side-chains. Shape memory testing by uniaxial deformation and recovery of molded tensile bars demonstrated that shape fixities greater than 96% and shape recoveries greater than 98% were obtained for extensional strains up to 300%. Although some loss of properties was observed with cycling, the entirely physically cross-linked nature of the polymer allowed erasing of the sample history and recovery of the initial properties by annealing the sample at elevated temperature.

KEYWORDS: shape memory polymer • block copolymer • octadecylacrylate • RAFT polymerization

INTRODUCTION

Shape memory polymers (SMPs) are a class of materials that can be deformed and set into a temporary shape and returned to their initial shape by the application of an external stimulus, such as an increase in temperature, exposure to ultraviolet light, or the absorption of water (1−8). This programmable movement makes them attractive as responsive materials, actuators, and sensors in fields including medicine, textiles, and aerospace (9−11).

In the majority of SMPs, the shape memory effect is obtained through a transition between a cross-linked glassy or semicrystalline thermoplastic and a cross-linked elastomer (5, 6). The deformation of the elastomer is set in the material by vitrification through crystallization or a glass transition, whereas the cross-linking prevents relaxation of the chains and provides the restoring force for recovering the initial shape.

Two general types of thermally responsive SMPs are AB block copolymers and chemically cross-linked side-chain crystalline copolymers (12−25). AB block copolymers are well-known to microphase separate into periodic nanostructures with A-rich and B-rich domains (26). When these polymers contain three or more blocks (ABA to $(AB)_n$ multiblock), the bridging and immobilization of the rubbery B chains across dispersed glassy or semicrystalline A domains generates a physically cross-linked polymer network that serves as the permanent network in the SMP (27). SMPs are obtained when the B domains have a glass transition or melting temperature in between the use temperature of the material and the transition temperature of the A domains. A key advantage of block copolymers for SMPs is their fabrication by melt and solution processing and their recyclability because of the lack of any covalent cross-linking (28−30).

SMPs are also generated by chemically cross-linking copolymer elastomers containing side-chain crystalline groups. Octadecylacrylate (stearyl acrylate) is a brittle thermoplastic, that is known to form side-chain crystals (31, 32). When copolymerized with a monomer such as methyl acrylate and a cross-linker, a chemically cross-linked elastomer is formed where the side-chain crystals act as additional physical cross-links (14). For SMPs, this approach provides two distinct advantages. First, the melting temperature and therefore transition temperature of the SMP can be precisely tuned over a range of ~15 °C by varying the concentration of side-chain crystalline repeat units. Second, the copolymer chemistry can be adjusted to form shape memory hydrogels and organogels through the swelling of the semicrystalline polymer (19).

This paper reports the shape memory behavior of a poly(styrene-*block*-methylacrylate-*random*-octadecylacrylate-*block*-styrene) (PS-*b*-PMA-*r*-PODA-*b*-PS) triblock copolymer. The copolymerization of PMA with PODA in the polymer midblock generates a material with two physically cross-linked networks, one from the block copolymer mesophase and the second from the dispersed side-chain crystals of PODA. As in the case of the chemically cross-linked PMA-*r*-PODA system, this random copolymer block is necessary. While a pure PS-*b*-PODA-*b*-PS polymer would act as a thermoplastic elastomer above the melting point of the

* Corresponding author. E-mail: kac58@uakron.edu. Phone: (330) 972-8368.
Received for review June 2, 2010 and accepted August 16, 2010

DOI: 10.1021/am100481p

PODA side-chain crystals, at room temperature a PS-*b*-PODA-*b*-PS polymer would be too brittle for use as an SMP. This polymer exhibited excellent shape memory properties. It can be extended up to 300% strain with fixities >96% and strain recovery >98%. Some loss of properties was observed with multiple cycles. However, after remolding these materials either by dissolution and casting or simply thermal annealing the sample history was erased and the initial properties were recovered. The uniqueness of this polymer is the advantageous combination of the physical cross-linking for utilizing polymer processing techniques, like molding, extrusion, and solvent casting and subsequent recycling and side-chain crystallinity for tuning the thermal properties.

EXPERIMENTAL METHODS

Materials. Methyl acrylate (MA) (99%, Acros) and styrene (99%, Acros) were passed through a column of activated basic aluminum oxide (Sigma-Aldrich) to remove the inhibitor. Octadecylacrylate (ODA) (Tokyo Kasei Kogyo CO., Ltd.) was purified by a previously reported method (33). ODA was dissolved in hexane and washed four times with 5% aqueous NaOH in a separatory funnel. After drying the organic phase over magnesium sulfate, the solution was passed through a column filled with neutral aluminum oxide (Sigma-Aldrich) and the solvent was removed under reduced pressure. The liquid ODA monomer was then crystallized at 8 °C in a refrigerator. α,α′-Azobis(isobutyronitrile) (AIBN) (98%, Sigma-Aldrich), p-toluenesulfonic acid monohydrate (98.5%, EMD Chemicals Inc.), tetrahydrofuran (99.5%, EMD Chemicals Inc.), hexane (99.9%, Fisher Scientific Co.), 1,6-hexanediol (97%, Alfa Aesar), cyclohexane (99.9%, Fisher Scientific Co.), benzene (99.0%, EMD Chemicals Inc.), methanol (99.9%, Fisher Scientific Co.), and silica gel 40 (0.063−0.200 mm, EMD Chemical Inc.) were all used as received.

Polymer Synthesis.

Synthesis of *S*-1-Dodecyl-*S*′-(α,α′-dimethyl-α″-acetic acid)trithiocarbonate. *S*-1-Dodecyl-*S*′-(α,α′-dimethyl-α″-acetic acid)trithiocarbonate was synthesized by a previously reported method (34).

Synthesis of Hexane-1,6-diyl di-(*S*-1-Dodecyl-*S*′-(α,α′-dimethyl-α″-acetic ester)trithiocarbonate) (di-DDMET). *S*-1-Dodecyl-*S*′-(α,α′-dimethyl-α″-acetic acid)trithiocarbonate (3 g, 8.24 mmol), 1,6-hexanediol (0.486 g, 4.11 mmol), *p*-toluenesulfonic acid (0.312 g, 1.64 mmol), and cyclohexane (3.528 g, 42 mmol) were placed in a 50 mL round-bottomed flask that was connected to a Dean−Stark trap, and a reflux condenser. The connecting tube between the flask and the trap was wrapped with glass wool. The trap was fully filled with cyclohexane. The flask was then placed in a thermostatted oil bath at 130 °C for 32 h. The resulting mixture was washed with distilled water three times. The organic phase was recovered, dried over magnesium sulfate, and the solvent was removed under reduced pressure. The product was then dissolved in benzene and passed through a column packed with silica gel. The solvent was removed under reduced pressure and the product was crystallized at −15 °C in a freezer. In this way, hexane-1,6-diyl di-(*S*-1-Dodecyl-*S*′-(α,α′-dimethyl-α″-acetic ester)trithiocarbonate) (2.49 g, 71.5% yield) was obtained as a yellow solid. δ_H (300 MHz, $CDCl_3$): 0.89 (t, 6H), 1.26−1.37 (m, 40H), 1.54−1.66 (m, 8H), 1.70 (s, 12H), 3.27 (t, 4H), 4.08 (t, 4H).

Synthesis of Poly(methylacrylate-*random*-octadecylacrylate) (PMA-*r*-PODA). ODA monomer (9.56 g, 30.25 mmol), di-DDMET (0.309 g, 0.38 mmol) and AIBN (25 mg, 0.15 mmol) were dissolved in MA monomer (10 mL, 111.16 mmol) in a 100 mL round-bottomed flask capped with a rubber septum and a magnetic stir bar to target a molecular weight of 50 kDa at 100% monomer conversion. The contents were sparged with nitrogen gas for 20 min. The sealed flask was then placed in a thermostatted oil bath at 60 °C for 6 h. The resulting mixture was dissolved in a small amount of tetrahydrofuran and precipitated in methanol followed by drying the polymer in a vacuum oven at room temperature overnight. PMA-*r*-PODA (17.7 g, 91.1% yield; M_n = 56396 g mol^{-1} compared to PS standards) was obtained as a yellow solid.

Synthesis of Poly(styrene-*block*-methylacrylate-*random*-octadecylacrylate-*block*-styrene) (PS-*b*-PMA-*r*-PODA-*b*-PS). The PMA-*r*-PODA (10 g, 0.18 mmol) was dissolved in styrene monomer (50 mL, 435.58 mmol) in a 500 mL round-bottomed flask. The contents were sparged with nitrogen gas for 20 min. The sealed flask was then placed in a thermostatted oil bath at 120 °C for 1 h. The resulting mixture was dissolved in a small amount of tetrahydrofuran and precipitated in methanol followed by drying the polymer in a vacuum oven at 100 °C overnight. In this way, PS-*b*-PMA-*r*-PODA-*b*-PS (13.9 g; M_n = 82761 g mol^{-1} compared to polystyrene standards) was obtained as a yellow solid.

Characterization.

Size Exclusion Chromatrography (SEC). SEC with tetrahydrofuran as the mobile phase was used to determine polymer molecular weights and polydispersity indices, using a Waters 1515 isocratic pump, three Waters Styragel columns (HR 3, HR 4, HR 4E), and a Waters 2414 refractive index detector. The GPC columns were calibrated with narrow-distribution polystyrene standards.

^{1}H NMR. Spectra were obtained using a Varian 300 MHz NMR spectrometer. Deuterated chloroform was used as the solvent.

Differential Scanning Calorimetry (DSC). A Q200 DSC, (TA Instruments) was used to study the thermal properties of the PMA-*r*-PODA and PS-*b*-PMA-*r*-PODA-*b*-PS samples. Samples were first heated to 200 at 10 °C/min and maintained at this temperature for 5 min. They were then cooled to −20 °C at a cooling rate of −10 °C/min by liquid nitrogen. Finally, they were heated to 200 °C again at a heating rate of 5 °C/min.

Wide-Angle X-ray Diffraction (WAXD). Exposures were taken at room temperature at a scan speed of 10°/min over the range of 5−35° using an X-ray diffractometer equipped with nickel-filtered Cu Kα radiation (40 KV, 40 mA) (Bruker AXS, Model D8 Discover).

Rheology. The rheological behavior of the PS-*b*-PMA-*r*-PODA-*b*-PS triblock was measured using a rms-800 rheometer (Rheometrics) with a parallel plate geometry (25 mm diameter). An isochronal temperature sweep was measured at a heating rate of 1 °C/min at a frequency of 0.1 rad/s. Isothermal frequency sweeps were measured at increments of 10 °C over the frequency range of 10 to 0.01 rad/s.

Bulk Mechanical Behavior. A uniaxial stress−strain curve was obtained at room temperature using an Instron 5567 tensile tester. Samples were cast from tetrahydrofuran into a dogbone mold. A extension rate of 10 mm/min was used.

Shape Memory Behavior. Cyclic loading tests were used to measure the fixity and recovery ratio of molded dogbone samples. An example procedure is as follows: A sample with an initial gauge length of L_1 was heated up to 65 °C in a hot water bath and held for 2 min, then stretched to a gauge length of L_2. The elongated sample was immediately quenched to 5 °C in a cold water bath and held at a constant length of L_2. It was then held at room temperature without any load for 10 min. A third gauge length of L_3 was measured. The cooled sample was then heated to 65 °C again in the hot water bath for 4 min to allow shape recovery. The recovered gauge length L_4 was measured. This procedure was repeated with the same sample five times. The following shape memory parameters were determined based on the measured gauge lengths L_1, L_2, L_3, and L_4

maximum strain (ε_m): $\varepsilon_m = \frac{L_2 - L_1}{L_1} \times 100\%$

fixed strain (ε_u): $\varepsilon_u = \frac{L_3 - L_1}{L_1} \times 100\%$

residual strain (ε_p): $\varepsilon_p = \frac{L_4 - L_1}{L_1} \times 100\%$

percent fixity (R_f): $R_f = \frac{\varepsilon_u}{\varepsilon_m} \times 100\%$

percent recovery (R_r): $R_r = \frac{\varepsilon_m - \varepsilon_p}{\varepsilon_m} \times 100\%$

The shape memory behavior was also tested using dynamic mechanical analysis (DMA Pyris Diamond, Perkin-Elmer) by controlling the stress and sample temperature and monitoring the resultant sample strain. A 5 mm length sample was placed in the DMA at room temperature. Six steps were executed to monitor the strain fixity and recovery: (1) an initial stress of 0.01 mN was set and the sample temperature was increased to 65 °C at a rate of 5 °C/min and held for 2 min; (2) the force on the sample was increased to 40 mN at a rate of 40 mN/min and held for 1 min; (3) the sample temperature was decreased to 0 °C at a cooling rate of 20 °C/min and held at 0 °C for 5 min; (4) the force was decreased to 0.01 mN at a rate of 20 mN/min and held for 1 min; (5) the temperature was increased to 65 °C at a heating rate of 1 °C/min and held at this temperature for 10 min.

RESULTS AND DISCUSSION

Polymer Structural Characterization. The SEC traces of the PMA-*r*-PODA and PS-*b*-PMA-*r*-PODA-*b*-PS copolymers are shown in Figure 1. Both traces exhibit monomodal, narrow peaks expected for a controlled free radical polymerization. The decrease in the peak elution time for the block copolymer compared to the precursor random copolymer is consistent with the increase in the molecular weight of the polymer from the addition of polystyrene blocks. The molecular weights and polydispersities of the polymers compared to polystyrene standards are listed in Table 1. Figure 2 shows the chemical structure of the triblock copolymer and its ^{1}H NMR spectra. The mole fractions of the styrene (S), methyl acrylate (MA), and octadecyl acrylate (ODA) repeat units were determined by integration of the nonoverlapping peaks corresponding to each chemically different repeat unit. The only nonoverlapping peaks from the RAFT agent are at 3.27 and 4.08 ppm. These peaks were not observed because of their low concentration in the high-molecular-weight polymer. The mole and weight fractions determined for each repeat unit are listed in Table 1.

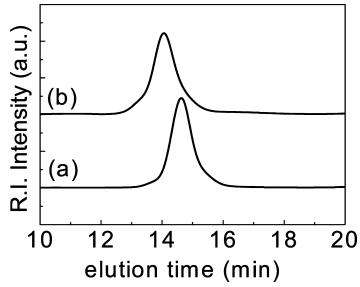

FIGURE 1. SEC traces of (a) the PMA-*r*-PODA random copolymer and (b) the PS-*b*-PMA-*r*-PODA-*b*-PS triblock copolymer.

Morphology Characterization. Figure 3 shows the DSC traces of the first cooling and second heating curves for the PMA-*r*-PODA and PS-*b*-PMA-*r*-PODA-*b*-PS block copolymer. The peaks are assigned to the crystallization and melting of the side-chain crystals formed by the ODA repeat units during cooling and heating, respectively. The melting and crystallization temperatures are listed in Table 1. The melting and crystallization temperatures of the PMA-*r*-PODA copolymers are similar to those previously measured for a chemically cross-linked PMA-*r*-PODA copolymer with a similar ODA mole fraction (T_m = 35 °C and T_c = 26 °C) (14). The reduction in the transition temperatures of the block copolymer compared to the random copolymer is attributed to the confinement of the PMA-*r*-PODA domains in the microphase separated block copolymer. A similar effect was observed in a PS-*b*-poly(octadecyl methacrylate) (PS-*b*-PODMA) block copolymer with PODMA cylinders and a glassy PS matrix when compared to the pure PODMA homopolymer (35).

The side-chain crystalline structure was further investigated using wide-angle X-ray diffraction (WAXD). Figure 4, shows the azimuthally averaged WAXD patterns for the random copolymer prior to the addition of the PS block, the block copolymer and a PS homopolymer. The peak at 21.3° corresponds to a domain spacing of 0.42 nm. This is consistent with the spacing between the extended side-chains previously measured in chemically cross-linked PMA-*r*-PODA (14). The other features are characteristic of the amorphous scattering from the PS and noncrystalline regions of the PMA-*r*-PODA blocks from comparison of the WAXD profiles.

The ordering transition of the triblock copolymer was investigated using a parallel plate rheometer. Figure 5 shows an isochronal temperature sweep at a frequency of 0.1 rad/s and a heating rate of 1 °C/min (Figure 5a) and isothermal frequency sweeps at different temperatures (Figure 5b, c). A small drop in G' and G'' is observed at 30−34 °C. This is assigned to the melting of the PODA side-chain crystals. A block copolymer order−disorder transition (ODT) has been

Table 1. Characteristics of PMA-*r*-PODA and PS-*b*-PMA-*r*-PODA-*b*-PS Polymers

polymer	M_n (kDa)	PDI	S (mol %)	ODA (mol %)	MA (mol %)	S (wt %)	ODA (wt %)	T_m	T_c
PMA-*r*-PODA	56	1.12	N/A	20	80	N/A	49	34	25
PS-*b*-PMA-*r*-PODA-*b*-PS	83	1.20	37	13	50	31	34	32	19

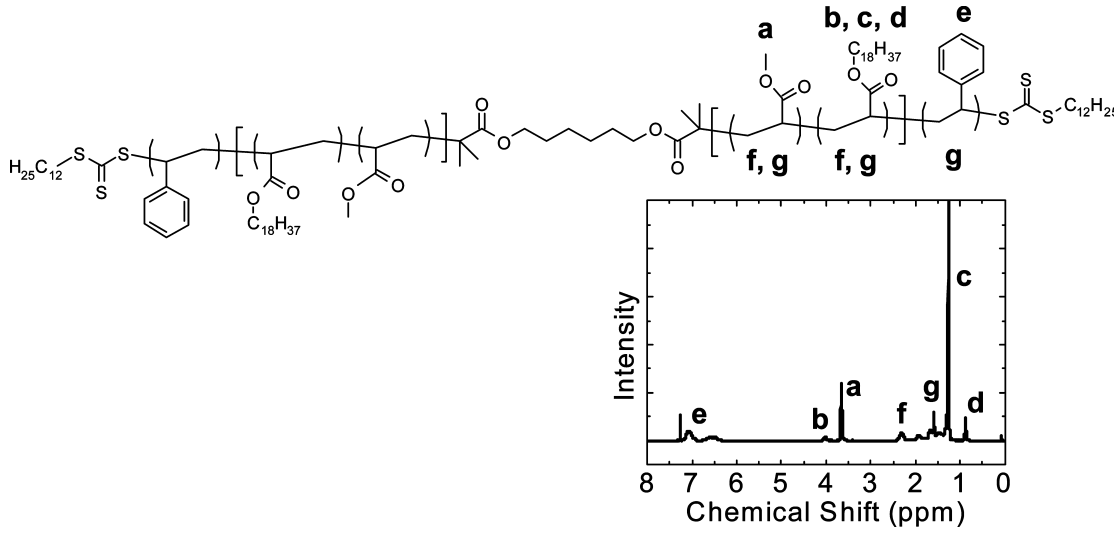

FIGURE 2. ^{1}H NMR spectra of the PS-*b*-PMA-*r*-PODA-*b*-PS triblock copolymer. The peaks arising from the side groups on (a) themethyl acrylate, (b−d) stearyl acrylate, and (e) styrene units, and from the backbone on the (f, g) acrylate and (g) styrene units are indicated.

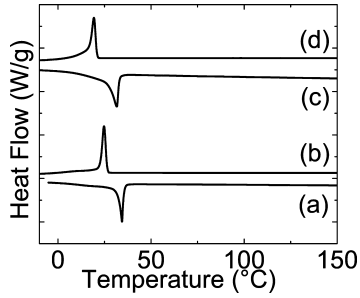

FIGURE 3. DSC traces for the PMA-*r*-PODA copolymer: (a) heating, (b) cooling; for PS-*b*-PMA-*r*-PODA-*b*-PS triblock copolymer: (c) heating, (d) cooling.

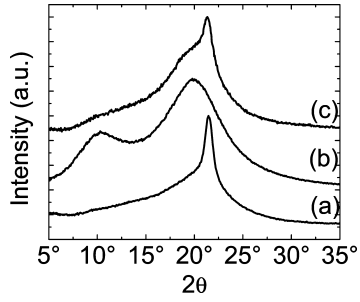

FIGURE 4. Azimuthally average WAXD intensity profile for (a) PMA-*r*-PODA, (b) PS, and (c) PS-*b*-PMA-*r*-PODA-*b*-PS triblock copolymer at room temperature.

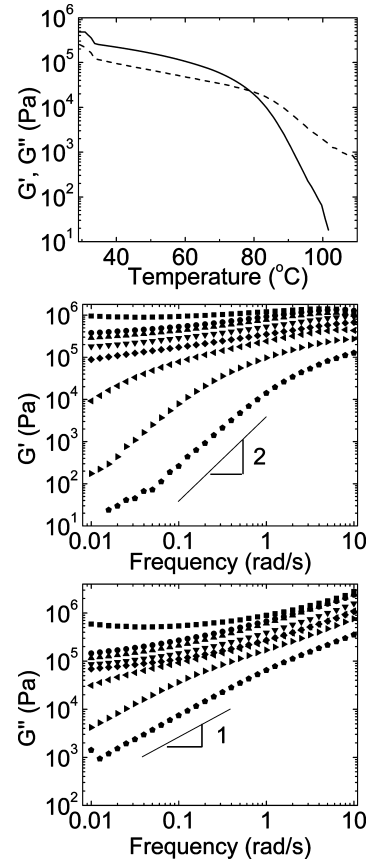

FIGURE 5. Rheology characterization.: (a) Isochronal temperature sweep: (solid line) G′, (dotted line) G″. (b) G′ vs ω: (square) 30 °C, (circle) 40 °C, (upward-facing triangle) 50 °C, (downward-facing triangle) 60 °C, (diamond) 70 °C, (left-facing triangle) 80 °C, (right-facing triangle) 90 °C, (pentagon) 100 °C. (c) G″ vs ω: the symbols are the same as in panel b.

found to correspond with a discontinuous drop in the storage, G', and loss, G'', moduli with temperature during an isochronal temperature sweep at low frequency (36). For both G' and G'' vs T, there is a change in slope around 80 °C. In the frequency sweeps, terminal behavior ($G' \approx \omega^2$, $G'' \approx \omega$) is observed above 80 °C, which is expected for a disordered block copolymer. Therefore, this polymer is a thermodynamically disordered liquid above 80 °C. The lack of very sharp transitions in the rheological data compared to other block copolymer systems may be due to an overlap of the glass transition temperature, T_g, of the polystyrene block and the order−disorder transition temperature, T_{ODT}. For a high-molecular-weight PS, $T_g = 100$ °C, this value is found to decrease with decreasing molecular weight at lower molecular weights due to the additional free volume provided by chain ends (37). The T_g is expected to be between 80−90 °C for PS molecular weights from 5−10 kDa. An estimate of the molecular weight of the PS blocks is 13.5 kDa, but the exact molecular weight of the PS end-blocks is unknown due to the uncertainty in the molecular weight of

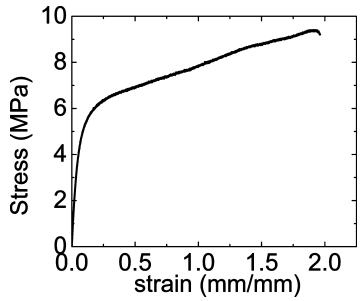

FIGURE 6. Uniaxial stress−strain curve of PS-*b*-PMA-*r*-PODA-*b*-PS at room temperature.

the PMA-*r*-PODA midblock, which was measured using PS standards. Additionally, the T_g can be depressed by interfacial mixing between the PMA-*r*-PODA and PS (38). For the thermodynamically disordered polymer the T_g can be estimated using the Fox equation

$$1/T_g = \sum w_i/T_{g,i}$$

where w_i and $T_{g,i}$ are the weight fractions and glass transition temperatures of the individual components of the polymer (39). The T_g of PODA is difficult to determine because of the side-chain crystallization, but has been estimated to be less than −80 °C (40). The T_g of PMA is 10 °C (41). An upper bound of the T_g is 33 °C, using $T_{g,PS}$ = 100 °C, $T_{g,PMA}$ = $T_{g,PODA}$ = 10 °C, and w_{PS} = 0.31, w_{PMA} = 0.35, and $w_{,PODA}$ = 0.34. During cooling, the sample would order at T_{ODT}. The vitrification of the PS domains during ordering would make it difficult to obtain long-range order. During heating, the system would be kinetically trapped until the T_g of the PS domains is reached, at which point the samples could undergo an order−disorder transition.

Bulk Mechanical and Shape Memory Behavior. The room-temperature mechanical behavior of the polymer was characterized by a uniaxial tension test. The stress−strain curve is shown in Figure 6. This polymer has a modulus of 13.8 MPa and can be extended to 200% strain before failure. Therefore, the copolymerization of PMA and PODA in the midblock produces a polymer that can easily be handled at room temperature.

The shape memory behavior was characterized by (1) uniaxially straining the samples in a hot water bath at 65 °C, (2) quenching the strained samples to 5 °C under load, (3) removing the load and holding the samples at room temperature for 10 min, and (4) reimmersing the samples into the 65 °C water bath. The gauge length of the sample was marked and measured before testing, and was measured after each step giving gauge lengths of L_1, L_2, L_3, and L_4 as described in the experimental section. Figure 7 shows the calculated percent fixity and percent recovery for three different strains (100, 200, and 300%) and five cycles of loading and recovery. For each cycle, a new initial gauge length, L_1, was measured. In addition, for the 100% strain, a sample was remolded after shape memory testing by annealing at 140 °C in the tensile bar mold and its shape memory properties were retested.

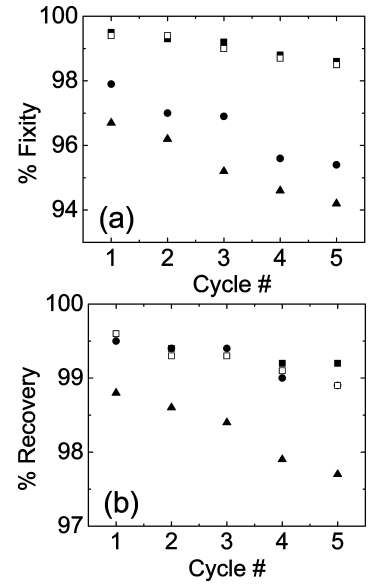

FIGURE 7. Unixaial shape memory tests. (a) % fixity vs cycle number: (■) 100% strain, (□) 100% strain, remolded, (●) 200% strain, (▲) 300% strain. (b) % recovery vs cycle number: the symbols are the same as in panel a.

During the first testing cycle, very good fixity and recovery properties are observed up to 300% strain. The differences in the fixity with strain are likely due to the small elastic recovery of the sample, which would be expected to be higher at larger strain. Some loss of recovery is also observed at 300% strain. One explanation is that there is some plastic deformation of the polystyrene domains. As these chains are short (~13.5 kDa) and near the entanglement molecular weight of PS, chain pull-out would be expected (42, 43). As the deformation and recovery are conducted below the T_g of PS, it would also be difficult for these pulled-out blocks to quickly reinsert into the PS domain and would therefore become elastically uneffective chains or defects in the permanent network. These defects also appear to affect the cycling of the material as a reduction in both the fixity and recovery is seen with increasing cycle number. However, these defects are not permanent, and can be healed by annealing the polymer at high temperature. This is evident from the overlap of the 100% strain data from the initial testing and after reannealing the sample.

The shape memory behavior was also characterized by dynamic mechanical analysis. Figure 8 shows the stress−strain−temperature plot using the procedure described in the experimental section. At this loading level a strain of 128% was obtained, which was reduced to 124% after cooling giving a shape fixity of 97%. On heating the strain recovery began at 26 °C, which corresponds to the onset of melting of the PODA side-chain crystals. However, the strain recovery behavior was completely different than the previous temperature jump experiments using water baths. First, the strain recovery took significantly longer. The 98−100% strain recoveries in the temperature jump experiments were obtained after four mintues of heating at 65 °C. Second, a strain recovery greater than 100% was observed.

To further investigate the behavior of the samples during DMA testing the following three experiments were per-

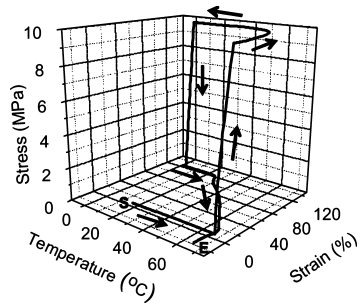

FIGURE 8. Stress−strain−temperature cycling of PS-*b*-PMA-*r*-PODA-*b*-PS block copolymer. On the plot, S indicates the start of the test and E indicates the end of the test.

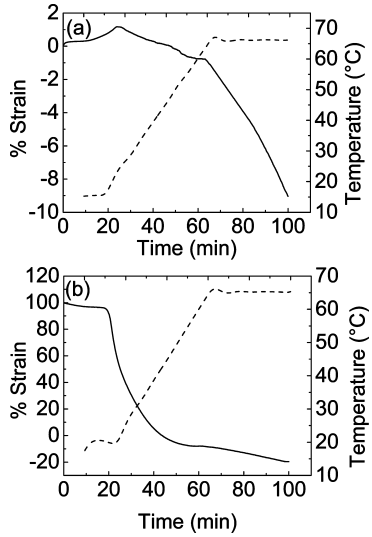

FIGURE 9. Sample strain vs time (solid line) during heating of PS-*b*-PMA-*r*-PODA-*b*-PS samples in the DMA: (a) undeformed sample, (b) prestrained to 100% strain. The temperature (dotted line) was increased at a rate of 1 °C/min.

formed. First, an undeformed sample was placed in the DMA and the temperature was ramped to 65 at 1 °C/min and then held at 65 °C. Second, a sample was strained to 100% using the hot and cold water baths as done previously and then its strain recovery was measured using the DMA. Third, a sample was deformed in the DMA and then removed after strain fixing and the strain recovery was tested by immersing the sample in a 65 °C water bath.

Figure 9a shows the results of the DMA experiment where an undeformed sample was heated. Initially the strain in the sample increased, likely because of thermal expansion of the sample. At 25 °C the strain starts to decrease. This transition coincides with the beginning of melting of the PODA side-chain crystals. It is apparent that this polymer is able to creep under its own weight in the DMA. Therefore, the strain recovery observed in Figure 8 also includes this sample creep and does not reflect the true strain recovery of the sample.

Figure 9b shows the results of the DMA experiment using a prestrained sample. The shape recovery appears significantly slower than in the samples that were instantaneously annealed at 65 °C by placing them in a water bath. As the temperature is increased the mobility of the polymer chains should also increase and therefore speed up the shape recovery. This sample also exhibited a greater than 100% strain recovery. This is attributed to the simultaneous creep of the sample during heating in the DMA instrument. To compare this long annealing time to the temperature jump experiments, a sample was deformed to 100% strain in a 65 °C water bath, quenched in ice water, and then placed back in the 65 °C water bath for 60 min. After annealing, a strain recovery of 100% was observed. This result is consistent with the greater than 100% strain recovery in the DMA measurement being due to sample creep.

For the third experiment, a maximum strain of 88% and a strain fixity of 97% were obtained after deformation in the DMA. After the sample was immersed in a 65 °C water bath for 5 min, a recovery ratio of 90% was obtained. The strain fixity and strain recovery are worse than were obtained in the 100% maximum strain samples using two water baths. This is attributed to the longer time spent at elevated temperature after strain fixing where the sample temperature was ramped down instead of quenched as in the water bath experiments. Here, some stress relaxation of the permanent block copolymer network could occur, which has previously been observed in ABA triblock copolymer thermoplastic elastomers at temperatures near the T_g of the glassy A domains (44).

Although these polymers exhibit good shape memory properties when processed using rapid temperature changes, the combination of stress relaxation and sample creep during longer-term annealing are detrimental to the characterization of the shape fixity and shape recovery kinetics of these materials. Increased resistance to stress relaxation and creep should be achieved by lowering the mobility of the ABA triblock copolymer. This could be accomplished by a number of means including increasing the molecular weight of the polymer, increasing the T_g of the glassy domains, and increasing the degree of segregation, χN, in the system, which would provide higher enthalpic barriers to motion (45). However, it should also be pointed out that although a reduction in the chain mobility could improve the characterization of these materials, it could affect their intrinsic properties beneficial for good shape memory behavior.

CONCLUSIONS

A new shape memory polymer was prepared from a triblock copolymer with glassy polystyrene end blocks and a random copolymer midblock of poly(methylacrylate) and poly(octadecylacrylate). This system combines the processability of block copolymers with the tunability of a side-chain crystalline crystalline copolymer to produce a unique shape memory material. This polymer exhibited good shape memory properties with shape fixities greater than 96% and shape recoveries greater than 98% for strains up to 300% using rapid temperature jumps during strain fixing and recovery. Some loss of properties was evident with repeated cycling. This was attributed to the pull-out of the chains from the polystyrene domains generating defects in the permanent network of the shape memory polymer. These defects could be completely healed by annealing the polymer at

temperatures above the T_g and T_{ODT} of the polymer. This side-chain crystalline, triblock copolymer architecture is suitable for the fabrication of shape memory materials. Future investigations will explore adjusting the shape memory properties through the structure of the block copolymer. Examples include using a multiblock copolymer architecture to prevent chain pull-out or adjusting the triggering temperature by varying the concentration of octadecylacrylate groups in the midblock. An additional area for improvement is in the sensitivity of the sample cycling to the annealing time where improvements in the resistance of the block copolymer network to stress relaxation and the sample to creep would allow more quantitative measurements of the strain fixing and recovery kinetics by dynamic mechanical analysis.

Acknowledgment. Acknowledgment is made to the University of Akron for the financial support of P.F.

REFERENCES AND NOTES

(1) Behl, M.; Lendlein, A. *Mater. Today* **2007**, *10*, 20–28.
(2) Dietsch, B.; Tong, T. *J. Adv. Mater.* **2007**, *39*, 3–12.
(3) Gunes, I. S.; Jana, S. C. *J. Nanosci. Nanotechnol.* **2008**, *8*, 1616–1637.
(4) Jiang, H.; Kelch, S.; Lendlein, A. *Adv. Mater.* **2006**, *18*, 1471–1475.
(5) Lendlein, A.; Kelch, S. *Angew. Chem., Int. Ed.* **2002**, *41*, 2034–2057.
(6) Liu, C.; Qin, H.; Mather, P. T. *J. Mater. Chem.* **2007**, *17*, 1543–1558.
(7) Ratna, D.; Karger-Kocsis, J. *J. Mater. Sci.* **2008**, *43*, 254–269.
(8) Rousseau, I. A. *Polym. Eng. Sci.* **2008**, *48*, 2075–2089.
(9) Lendlein, A. *Smart Fibres, Fabr. Clothing* **2001**, 278–290.
(10) Mondal, S.; Hu, J. L. *Indian J. Fibre Text. Res.* **2006**, *31*, 66–71.
(11) Sofla, A. Y. N.; Meguid, S. A.; Tan, K. T.; Yeo, W. K. *Mater. Des.* **2010**, *31*, 1284–1292.
(12) Jeong, H. M.; Lee, S. H.; Cho, K. J.; Jeong, Y. T.; Kang, K. K.; Oh, J. K. *J. Appl. Polym. Sci.* **2002**, *84*, 1709–1715.
(13) Jeong, H. M.; Song, J. H.; Chi, K. W.; Kim, I.; Kim, K. T. *Polym. Int.* **2002**, *51*, 275–280.
(14) Kagami, Y.; Gong, J. P.; Osada, Y. *Macromol. Rapid Commun.* **1996**, *17*, 539–543.
(15) Lee, H. Y.; Jeong, H. M.; Lee, J. S.; Kim, B. K. *Polym. J.* **2000**, *32*, 23–28.
(16) Li, F.; Zhang, X.; Hou, J.; Xu, M.; Luo, X.; Ma, D.; Kim, B. K. *J. Appl. Polym. Sci.* **1997**, *64*, 1511–1516.
(17) Luo, X.; Zhang, X.; Wang, M.; Ma, D.; Xu, M.; Li, F. *J. Appl. Polym. Sci.* **1997**, *64*, 2433–2440.
(18) Min, C.; Cui, W.; Bei, J.; Wang, S. *Polym. Adv. Technol.* **2005**, *16*, 608–615.
(19) Mitsumata, T.; Gong, J. P.; Osada, Y. *Polym. Adv. Technol.* **2001**, *12*, 136–150.
(20) Nagata, M.; Kitazima, I. *Colloid Polym. Sci.* **2006**, *284*, 380–386.
(21) Osada, Y.; Matsuda, A. *Nature* **1995**, *376*, 219.
(22) Reyntjens, W. G.; Du Prez, F. E.; Goethals, E. J. *Macromol. Rapid Commun.* **1999**, *20*, 251–255.
(23) Takahashi, T.; Hayashi, N.; Hayashi, S. *J. Appl. Polym. Sci.* **1996**, *60*, 1061–1069.
(24) Sakurai, K.; Tanaka, H.; Ogawa, N.; Takahashi, T. *J. Macromol. Sci., Phys.* **1997**, *B36*, 703–716.
(25) Ikematsu, T.; Kishimoto, Y.; Karaushi, M. Block copolymer bumpers with good shape memory. Japan Patent 02022355, 1990.
(26) Hamley, I. W. *The Physics of Block Copolymers*; Oxford University Press: New York, 1998.
(27) Spontak, R. J.; Patel, N. P. *Curr. Opin. Colloid Interface Sci.* **2000**, *5*, 334–341.
(28) Cha, D. I.; Kim, H. Y.; Lee, K. H.; Jung, Y. C.; Cho, J. W.; Chun, B. C. *J. Appl. Polym. Sci.* **2005**, *96*, 460–465.
(29) Chen, S.; Hu, J.; Zhuo, H.; Zhu, Y. *Mater. Lett.* **2008**, *62*, 4088–4090.
(30) Ji, F.; Zhu, Y.; Hu, J.; Liu, Y.; Yeung, L.-Y.; Ye, G. *Smart Mater. Struct.* **2006**, *15*, 1547–1554.
(31) Greenberg, S. A.; Alfrey, T. *J. Am. Chem. Soc.* **1954**, *76*, 6280–6285.
(32) Mogri, Z.; Paul, D. R. *J. Membr. Sci.* **2000**, *175*, 253–265.
(33) Qin, S.; Saget, J.; Pyun, J.; Jia, S.; Kowalewski, T.; Matyjaszewski, K. *Macromolecules* **2003**, *36*, 8969–8977.
(34) Lai, J. T.; Filla, D.; Shea, R. *Macromolecules* **2002**, *35*, 6754–6756.
(35) Hempel, E.; Budde, H.; Horning, S.; Beiner, M. *Thermochim. Acta* **2005**, *432*, 254–261.
(36) Rosedale, J. H.; Bates, F. S. *Macromolecules* **1990**, *23*, 2329–2338.
(37) Fox, T. G.; Flory, P. J. *J. Polym. Sci.* **1954**, *14*, 315–319.
(38) Robertson, C. G.; Hogan, T. E.; Rackaitis, M.; Puskas, J. E.; Wang, X. *J. Chem. Phys.* **2010**, *132*, 104904.
(39) Fox, T. G. *Bull. Am. Phys. Soc.* **1956**, *1*, 123.
(40) Giotto, M.; Azar, D.; Gosselin, J.; Inglefield, P. T.; Jones, A. A. *J. Polym. Sci., Part B: Polym. Phys.* **2001**, *39*, 1548–1552.
(41) Schneider, H. A. *Polymer* **2005**, *46*, 2230–2237.
(42) Creton, C.; Brown, H. R.; Shull, K. R. *Macromolecules* **1994**, *27*, 3174–3183.
(43) Fetters, L. J.; Lohse, D. J.; Richter, D.; Witten, T. A.; Zirkel, A. *Macromolecules* **1994**, *27*, 4639–4647.
(44) Mandare, P.; Horst, R.; Winter, H. H. *Rheol. Acta* **2005**, *45*, 33–41.
(45) Cavicchi, K. A.; Lodge, T. P. *Macromolecules* **2003**, *36*, 7158–7164.

AM100481P